Radboud Repository

Radboud University Nijmegen

PDF hosted at the Radboud Repository of the Radboud University Nijmegen

The following full text is a publisher's version.

For additional information about this publication click this link.
http://hdl.handle.net/2066/32748

Please be advised that this information was generated on 2021-09-21 and may be subject to change.

Modeling the Phase Diagram of Carbon

Luca M. Ghiringhelli,[1] Jan H. Los,[2] Evert Jan Meijer,[1] A. Fasolino,[1,2] and Daan Frenkel[1,3]
[1]*van 't Hoff Institute for Molecular Sciences, Universiteit van Amsterdam, Nieuwe Achtergracht 166, 1018 WV Amsterdam, The Netherlands*
[2]*Theoretical Physics, IMM, Radboud University Nijmegen, Toernooiveld, 6525 ED Nijmegen, The Netherlands*
[3]*FOM Institute for Atomic and Molecular Physics, Kruislaan 407, 1098 SJ, Amsterdam, The Netherlands*

(Received 9 December 2004; published 13 April 2005)

We determined the phase diagram involving diamond, graphite, and liquid carbon using a recently developed semiempirical potential. Using accurate free-energy calculations, we computed the solid-solid and solid-liquid phase boundaries for pressures and temperatures up to 400 GPa and 12 000 K, respectively. The graphite-diamond transition line that we computed is in good agreement with experimental data, confirming the accuracy of the employed empirical potential. On the basis of the computed slope of the graphite melting line, we rule out the hotly debated liquid-liquid phase transition of carbon. Our simulations allow us to give accurate estimates of the location of the diamond melting curve and of the graphite-diamond-liquid triple point.

DOI: 10.1103/PhysRevLett.94.145701 PACS numbers: 64.70.−p, 34.20.Cf, 61.20.Ja

Knowledge of the phase diagram of carbon under extreme conditions is of crucial importance for a better understanding of a wide variety of physical phenomena. This phase diagram determines the carbon content of the interior of the earth and other planets and it determines the optimal conditions for the manufacturing of synthetic diamonds. In spite of intensive experimental, theoretical, and numerical investigations [1–15], our knowledge of the phase diagram of carbon for pressures (P) and temperatures (T) in the range up to 100 GPa and 10 000 K is still fragmented because experiments under these conditions are difficult if not outright impossible. Thus far, quantitative theoretical and numerical predictions were hampered by the fact that the existing atomistic models for carbon had serious flaws that made them unsuited for quantitative predictions. In this Letter, we show that free-energy calculations [16] on a recently proposed model for carbon [17] allows us to compute the carbon phase diagram with unprecedented accuracy.

In the range of pressures and temperatures up to 100 GPa and 10 000 K, carbon exhibits a graphite (G) and a diamond (D) solid phase at lower temperatures, and a liquid (L) phase at higher temperatures (Figs. 1 and 2). The graphite-diamond coexistence line has been relatively well characterized up to 2400 K [1,8]. For the graphite melting line, a large amount of experimental data are available [2–4,6,7,9]. The experiments have in common that the melting temperature varies little with pressure, and most of the measured graphite melting $P - T$ lines [2,3,9] show a maximum around $P = 6$ GPa. However, the nature of the maximum is not well established. The melting temperatures show a rather large spread. In any event, as was pointed out in Ref. [15], these melting temperatures are determined indirectly, on the basis of a rather uncertain estimate of the melting temperature at ambient pressure. It appears that the estimated melting temperature depends significantly on the heating rate of the sample [6,7], yielding values from 3700 to 5000 K below 0.01 GPa. The precise nature of the maximum in the melting curve is important, because a discontinuous change of slope of the melting curve at this point would imply the existence of a liquid-liquid phase transition (LLPT) line, branching off from the graphite melting curve.

The possible existence of a LLPT for carbon has been the object of much speculation. After the theoretical analysis of Ref. [10], based on the experimental data of Ref. [2], the question of a pressure-driven first-order transition in the graphite melt was addressed. In subsequent theoretical work [11], it was suggested that the transition takes place between two liquid phases, from a dominantly sp_2-coordinated (threefold) to a denser, mainly sp_3-coordinated (fourfold) liquid. The strain energy among the two liquid would be large enough, according

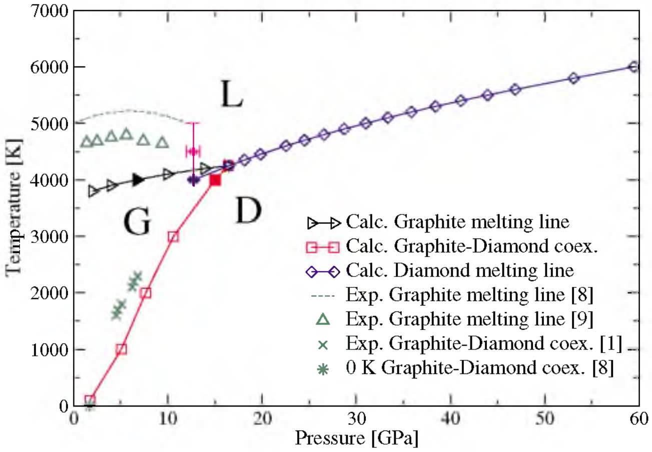

FIG. 1 (color online). Phase diagram of carbon at lower pressure. The solid triangle, square, and diamond are the three coexistence points found by equating the chemical potentials at 4000 K (see text). The solid circle with error bars indicates the experimental estimate for the L-G-D triple point [8,11,13].

0031-9007/05/94(14)/145701(4)$23.00

© 2005 The American Physical Society

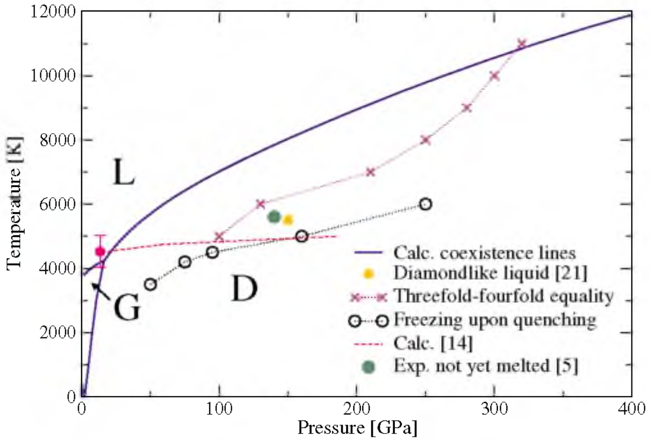

FIG. 2 (color online). Phase diagram of carbon at all calculated pressure. Solid circle, shock-wave experiment of Ref. [5] indicating diamond. Crosses mark the liquid with equal amount of three and fourfold atoms. Circles represent state points in which the sample freezes. In the region in between the two series is the "diamondlike liquid": the star is the point reported in Ref. [21].

to Refs. [18,19], to allow a first-order LLPT. Molecular dynamics (MD) simulations [13] with the semiempirical Brenner bond-order potential [20] found indeed a first-order LLPT, albeit between a mainly twofold liquid and a mainly fourfold liquid. Subsequent *ab initio* MD simulations [15,21] did not confirm this finding. Rather, these authors suggested that an overestimation of the torsional contributions in the model potential of Ref. [13] was responsible for the transition.

In shock-wave experiments [5] it was found that at $P = 140$ GPa (solid circle in Fig. 2) the diamond sample was not yet melted at a temperature beyond the triple point temperature, implying that the carbon diamond melting line has a positive slope in the $P - T$ diagram. The diamond melting line for the Brenner bond-order potential (dashed line in Fig. 2), obtained by computer simulation [14], also shows a positive slope. However, comparison with the shock-wave experiment at 140 GPa indicates that the Brenner model underestimates the diamond melting temperature.

Realistic modeling of the carbon phase diagram involving liquid, graphite, and diamond requires an accurate description of the interatomic interactions, combined with a precise evaluation of the relative stability of the involved phases. In practice, the latter requires the evaluation of the free energy of state points in all phases involved. The Brenner bond-order potential does not provide an accurate description of graphite since it does not account for the interactions among the planar sheets. Presently, density-functional theory based *ab initio* MD simulations would provide the best possible approach. However, for carbon, such an approach would be prohibitively expensive, in particular, when combined with free-energy calculations. Recently, some of us [17,21] proposed a semiempirical long-range carbon bond-order potential (LCBOP) that is partly based on *ab initio* data. This is the first empirical potential that is capable of providing an accurate description of all phases involved. The LCBOP accounts for the interplanar interactions in graphite, and it closely matches the *ab initio* MD results for the liquid structure of carbon [21]. This makes the LCBOP uniquely suited to predict the carbon phase diagram. The present Letter reports the phase diagram of LCBOP carbon up to $T = 12\,000$ K and $P = 400$ GPa. Note that at pressures and temperatures much higher than considered here carbon may form structures with higher coordination numbers [22]. Proper modeling of that region of the phase diagram may require an adaption of the LCBOP.

The properties of the liquid, graphite, and diamond phases were determined by Monte Carlo simulations. Coexistence lines were determined by locating points in the $P - T$ diagram with equal chemical potential for the two phase involved. To this purpose, we first determined the chemical potential for liquid, graphite, and diamond at an initial state point ($P = 10$ GPa, $T = 4000$ K). Subsequently, the L-G, L-D, and G-D coexistence pressures at $T = 4000$ K were located. In turn, these coexistence points served as the starting point for the determination of the graphite melting, diamond melting, and G-D coexistence lines, obtained integrating the Clausius-Clapeyron equation ($dT/dP = T\Delta v/\Delta h$, where Δv is the difference in specific volume, and Δh the difference in molar enthalpy between the two phases).

For all phases, the free energies at the initial state point F^* were determined by transforming the systems into a reference system $F^{\rm ref}$ of known free energy, using $U_\lambda = (1 - \lambda)U^* + \lambda U^{\rm ref}$. Here, U^* and $U^{\rm ref}$ denote the potential energy function of the LCBOP and the reference system, respectively. The transformation is controlled by varying the parameter λ from 0 to 1. The free-energy change upon the transformation was determined by thermodynamic integration:

$$F^* = F^{\rm ref} + \int_0^1 d\lambda \langle U^{\rm ref} - U^* \rangle_\lambda. \qquad (1)$$

The symbol $\langle \ldots \rangle_\lambda$ denotes the ensemble average with the potential U_λ.

For the liquid phase the reference system was taken to be a Lennard-Jones 12-6 (LJ) system. The LJ liquid free energy has been accurately parametrized [23]. The LJ ϵ parameter was chosen such that at $T = 4000$ K the LJ liquid was above the critical temperature. The LJ σ parameter was determined by matching the first peak of the radial distribution functions of the LCBOP and the LJ liquid at the same position, ensuring optimal similarity between the structure of the two liquids. For the solid phases the Einstein crystal was taken as the reference system [24]. The Einstein crystal spring constant was fixed in such a way that the mean-squared displacement from the equilibrium lattice positions of the Einstein crystal and the LCBOP are equal.

The chemical potential μ along the 4000 K isotherm was obtained by integrating from the initial state point a fit, $P(\rho) = a + b\rho + c\rho^2$, through simulated (P, T) state points along the 4000 K isotherm. Here, ρ is the number density, and a, b, and c are fit parameters. This yields for the chemical potential [25]

$$\beta\mu(\rho) = \frac{\beta F^*}{N} + \beta\left(\frac{a}{\rho^*} + b\ln\frac{\rho}{\rho^*} + b + c(2\rho - \rho^*)\right). \tag{2}$$

Here, ρ^* denotes the number density at the initial state point, N the number of particles, and $\beta = 1/k_BT$, with k_B the Boltzmann constant.

Monte Carlo simulations were performed for systems of 216 carbon atoms. For graphite, the atoms were placed in a periodic rectangular box with an edge-size ratio of about 1:1.5:1.7. For the liquid phase and diamond a periodic cubic box was used. State points for the 4000 K isotherm and the coexistence lines were obtained by constant pressure simulations. State points for the evaluation of Eq. (1) were simulated at constant volume. In the evaluation of the thermodynamic integration of Eq. (1) we used a ten-point Gauss-Legendre scheme. The parameters σ and ϵ for the LJ fluid were 0.127 nm and 31.84 kJ/mol. The Einstein crystal spring constant was set to 453 000 and 39 700 $\mathrm{kJ/(mol\,nm^2)}$ for graphite and diamond, respectively. The free energies $\beta F^{\mathrm{ref}}/N$ were -10.863, -5.755, and -1.912 for the liquid, graphite, and diamond reference systems, respectively. The integration in Eq. (1) yields for $\beta F^*/N$: -25.137 ± 0.002, -25.090 ± 0.006, and -24.583 ± 0.002. The fit parameters [a/GPa, $b/(\mathrm{GPa\,nm^3})$, $c/(\mathrm{GPa\,nm^6})$] in Eq. (2) yield values of (89.972, 1.9654, 0.011 092), (74.809, 3.6307, 0.019 102), (108.29, 2.2707, 0.011 925).

The three curves, μ_L, μ_G, μ_D, as given in formula (2), intersect in pairs in three points (these points are shown as a solid triangle, square, and diamond in Fig. 1). The intersections locate the G-L coexistence at 6.72 ± 0.60 GPa ($\mu_{GL} = -24.21 \pm 0.10 k_BT$), and the G-D coexistence at 15.05 ± 0.30 GPa ($\mu_{GD} = -23.01 \pm 0.03 k_BT$). The third intersection locates a D-L coexistence at = 12.75 ± 0.20 GPa ($\mu_{DL} = -23.24 \pm 0.03 k_BT$). Even though both the diamond and the liquid are there metastable, this point can be taken as the starting one for the Clausius-Clapeyron integration of the diamond melting line. Starting from the three coexistence points at 4000 K, the coexistence lines were traced by integrating the Clausius-Clapeyron equation using the trapezoidal-rule predictor-corrector scheme [26].

The calculated phase diagram in the $P - T$ plane is shown in Fig. 1 for the low pressure region, and in Fig. 2 for the full range of pressures and temperatures considered. Table I lists the densities of selected points on the coexistence lines. The three coexistence lines meet in a triple point at 16.4 ± 0.7 GPa and 4250 ± 10 K. The G-D coexistence line agrees very well with the experimental data. In the region near the L-G-D triple point, which has not been directly probed in experiments, the G-D coexistence line bends to the right, departing from the usually assumed straight line [8]. Analysis of our data shows this is mainly due to the fast reduction with increasing pressure of the interplanar distance in graphite at those premelting temperatures. This causes an enhanced increase of the density in graphite, yielding a decrease of dT/dP.

The calculated graphite melting line is monotonically increasing in a small temperature range around 4000 K. In contrast to data inferred from experiments, it shows no maximum and is at a somewhat lower temperature. In agreement with the experiments, the coexistence temperature is only slowly varying with pressure. Inspection reveals that this behavior is due to (i) the limited variability of the melting enthalpy, and (ii) a similar bulk modulus for liquid and graphite such that Δv is almost constant.

The slope of the diamond melting line is consistent with the only experimental point available [5] (see Fig. 2). When compared to the diamond melting line of the Brenner model [14], the LCBOP diamond melting line has a steeper slope yielding significantly higher temperatures for the diamond melting line. The other important distinction from the Brenner potential is that the LCBOP exhibits no liquid-liquid transition near the graphite melting line [13], consistent with the *ab initio* MD simulations [15,21], tight-binding MD simulations [27], and MD simulations employing an improved Brenner potential [28]. We found that, in the liquid near the graphite melting line, the coordination was rather constant with dominant threefold coordination, and a small fraction of twofold coordinated atoms. Only a tiny fraction of fourfold coordinated structures appears at densities near the triple point. Along the diamond melting line, from the triple point up to 400 GPa, the threefold coordinated atoms are gradually replaced by fourfold coordinated atoms. However, only at 300 GPa, 10 500 K does the liquid have an equal fraction of threefold

TABLE I. Pressure (P), temperature (T), and solid and liquid densities (ρ) along the melting lines.

Graphite melting line

P [GPa]	T [K]	ρ_G [10^{-3} kg/m^3]	ρ_L [10^{-3} kg/m^3]
2.0	3800	2.134	1.759
6.7	4000	2.354	2.098
16.4	4250	2.623	2.414

Diamond melting line

P [GPa]	T [K]	ρ_D [10^{-3} kg/m^3]	ρ_L [10^{-3} kg/m^3]
16.4	4250	3.427	2.414
25.5	4750	3.470	2.607
43.9	5500	3.558	2.870
59.4	6000	3.629	3.043
99.4	7000	3.783	3.264
148.1	8000	3.960	3.485
263.2	10 000	4.286	3.868
408.1	12 000	4.593	4.236

and fourfold coordinated atoms. These results contradict the generally assumed picture (see, e.g., Ref. [11]) that diamond melts into a fourfold coordinated liquid.

We determined the properties of the metastable liquid along the graphite melting line in the diamond region. Figure 2 shows the liquid $P-T$ state points (crosses) that exhibit an equal number of three and fourfold coordinated atoms. It ranges from the high-pressure, high-temperature region where the liquid is thermodynamically stable down into the diamond region, where the liquid is metastable for the LCBOP. The circles indicate state points in which the LCBOP liquid freezes in the simulation. Between the two sets of points lies the diamondlike liquid addressed in Ref. [21]. This liquid shows a mean square displacement much lower than the mainly threefold liquid, and a diamondlike structure in the first coordination shell. This suggests that a (meta)stable liquid with a dominantly fourfold coordination may exist only for pressures beyond ≈ 100 GPa. This could imply that the freezing of liquid into a diamond structure might be severely hindered for a large range of pressures beyond the L-G-D triple point. In Ref. [21] it is also pointed out that at 6000 K the equation of state shows a change of slope around the transition to the fourfold liquid. At even lower temperatures this feature becomes more and more evident, but for temperatures lower than ~4500 K the liquid freezes into a mainly fourfold coordinated amorphous structure. This observation is consistent with quenching MD simulations [29,30] to obtain the tetrahedral amorphous carbon. In those simulations a mainly threefold liquid freezes into an almost completely fourfold amorphous.

In summary, using an accurate semiempirical bond-order potential (LCBOP) we could predict the carbon phase diagram comprising graphite, diamond, and the liquid. We found the graphite-diamond line in good agreement with experimental data, confirming the accuracy of the LCBOP. The slope of the calculated graphite melting line, where experimental data are of limited accuracy, provides evidence against the existence of a possible liquid-liquid phase transition. Furthermore, even at higher pressure along the diamond melting line, no signal of such a transition was found. Our results for the graphite-diamond-liquid triple point and the diamond melting line may be considered the most accurate prediction to date. The calculated phase diagram provides a starting point for studying the (kinetics of) nucleation of liquid carbon, of importance in the area of geophysics and astrophysics, and the synthetic manufacturing of extremely robust compounds.

This work is part of the research program of the "Stichting voor Fundamenteel Onderzoek der Materie (FOM)," which is financially supported by the "Nederlandse Organisatie voor Wetenschappelijk Onderzoek (NWO)." J. H. L. and A. F. acknowledge NWO project 015.000.031 for financial support. E. J. M. acknowledges the Royal Netherlands Academy of Art and Sciences for financial support. We acknowledge support from the Stichting Nationale Computerfaciliteiten (NCF) and the Nederlandse Organisatie voor Wetenschappelijk Onderzoek (NWO) for the use of supercomputer facilities. L. M. G. wishes to thank Daniele Moroni for useful discussions.

[1] F. P. Bundy, H. P. Bovenkerk, H. M. Strong, and J. R. H. Wentorf, J. Chem. Phys. **35**, 383 (1961).
[2] F. P. Bundy, J. Chem. Phys. **38**, 618 (1963).
[3] N. S. Fateeva and L. F. Vereshchagin, Pis'ma Zh. Eksp. Teor. Fiz. **13**, 157 (1971) [JETP Lett. **13**, 110 (1971)].
[4] A. G. Whittaker, Science **200**, 763 (1978).
[5] J. W. Shaner, J. M. Brown, A. C. Swenson, and R. G. McQueen, J. Phys. (Paris), Colloq. **45**, C8-235 (1984).
[6] E. I. Asinovskii, A. V. Kirillin, and A. V. Kostanovskii, High Temp. **35**, 704 (1997).
[7] E. I. Asinovskii, A. V. Kirillin, A. V. Kostanovskii, and V. E. Fortov, High Temp. **36**, 716 (1998).
[8] F. P. Bundy, W. A. Bassett, M. S. Weathers, R. J. Hemley, H. K. Mao, and A. F. Goncharov, Carbon **34**, 141 (1996).
[9] M. Togaya, Phys. Rev. Lett. **79**, 2474 (1997).
[10] I. A. Korsunskaya, D. S. Kamenetskaya, and I. L. Aptekar, Fiz. Met. Metalloved. **34**, 942 (1972) [Phys. Met. Metallogr. (USSR) **34**, 39 (1972)].
[11] M. van Thiel and F. H. Ree, Phys. Rev. B **48**, 3591 (1993).
[12] L. E. Fried and W. M. Howard, Phys. Rev. B **61**, 8734 (2000).
[13] J. N. Glosli and F. H. Ree, Phys. Rev. Lett. **82**, 4659 (1999).
[14] J. N. Glosli and F. H. Ree, J. Chem. Phys. **110**, 441 (1999).
[15] C. J. Wu, J. N. Glosli, G. Galli, and F. H. Ree, Phys. Rev. Lett. **89**, 135701 (2002).
[16] D. Frenkel and B. Smit, *Understanding Molecular Simulation* (Academic Press, San Diego, CA, 2002).
[17] J. H. Los and A. Fasolino, Phys. Rev. B **68**, 024107 (2003).
[18] E. Rapoport, J. Chem. Phys. **46**, 2891 (1967).
[19] S. Strässler and C. Kittel, Phys. Rev. **139**, A758 (1965).
[20] D. W. Brenner, Phys. Rev. B **42**, 9458 (1990); **46**, 1948(E) (1992).
[21] L. M. Ghiringhelli, J. H. Los, E. J. Meijer, A. Fasolino, and D. Frenkel, Phys. Rev. B **69**, 100101 (2004).
[22] M. P. Grumbach and R. M. Martin, Phys. Rev. B **54**, 15 730 (1996).
[23] J. K. Johnson, J. A. Zollweg, and K. E. Gubbins, Mol. Phys. **78**, 591 (1993).
[24] D. Frenkel and J. C. Ladd, J. Chem. Phys. **81**, 3188 (1984).
[25] J. Anwar, D. Frenkel, and M. G. Noro, J. Chem. Phys. **118**, 728 (2003).
[26] D. A. Kofke, J. Chem. Phys. **98**, 4149 (1993).
[27] J. C. Morris, C. Z. Wang, and K. M. Ho, Phys. Rev. B **52**, 4138 (1995).
[28] O. Kum, F. H. R. S. J. Stuart, and C. J. Wu, J. Chem. Phys. **119**, 6053 (2003).
[29] N. A. Marks, J. Phys. Condens. Matter **14**, 2901 (2002).
[30] N. A. Marks, N. Cooper, D. R. McKenzie, D. G. McCulloch, P. Bath, and S. P. Russo, Phys. Rev. B **65**, 075411 (2002).